Copper Electroplating Parameters Optimisation

L.M.A. Ferreira*, CERN , Geneva, Switzerland
*Corresponding author: CERN, CH-1211 Geneva 23, leonel.ferreira@cern.ch

Abstract: Copper electroplating is a well-known and widely used industrial surface finishing process, however it becomes less attainable when complex geometries meet tight tolerances. The work presents a copper plating process for an accelerator component, which was modelled via the COMSOL Multiphysics® Electrodeposition Module. The objective was to evaluate two existing copper plating baths and their impact on the current density distribution and other plating parameters. Only electrochemical parameters were taken into account.

Keywords: Electroplating, current density, thickness distribution.

1. Introduction

Particle accelerators can go from relatively small equipment such as cathodic tubes, present in old television devices, to medium size (several meters) for medical applications or up to very large (several kilometres), dedicated to fundamental or applied R&D. Present and future very large machines rely on superconducting devices such as accelerating radio frequency (SCRF) cavities or magnets. Present superconducting materials operate near zero Kelvin; this very low temperatures have also an impact on the design of nearby non superconducting equipment, such as the couplers. The performance of these superconducting structures fully outcomes the construction and operating costs of the inherent cryogenics services.

Power couplers interfere directly with SCRF devices as they are responsible for: transfer the RF power to the cavity and match the impedance; bridge the gap between room and cryogenic temperature; provide a vacuum barrier for the beam vacuum. Besides a stainless steel structural and mechanical assembly, a copper coating is necessary on certain surfaces of a coupler. This copper layer provides: high electrical conductivity for low resistive RF losses and less heating (high RRR); low thermal conductance for low static cryogenic losses (thin layer). The layer must have: a good uniformity of thickness; low surface roughness to avoid field enhancement and no peel off to avoid contamination of the SCRF device.

Aqueous based copper electroplating seems the most reliable, flexible, cost effective method to create this copper layer on stainless steel base material structures; this however, doesn't imply a straightforward application, as the coupler geometry is complex and tolerances are tight. At CERN, two existing copper electroplating baths were tested to evaluate the feasibility of plating three couplers subcomponents within the demanded dimensional tolerances. COMSOL Multiphysics® Electrodeposition Module was used to optimise the counter electrode geometry with the objective of achieving an as even as possible copper layer thickness, as well as obtaining the plating parameters such as applied current density and plating time.

2. Physics and assumptions

An electrochemical cell is characterised by the relation between the current that passes and the applied voltage. This relation depends on various physical phenomena in the electrodes, in the electrolyte and at the interface between them.

In the electrolyte, the current density vector can be given by the Nernst-Planck equation by incorporating the current density expression, see equation 1:

$$i_l = -F(\nabla \sum_i z_i D_i c_i) - F^2 \nabla \phi_l \sum_i z_i^2 u_{m,i} c_i + uF \sum_i z_i c_i \quad (1)$$

where i_l stands for current density vector in the electrolyte, F the Faraday constant, z_i the charge number of each ion, D_i the diffusion coefficient, c_i the concentration of each ion, ϕ_l the electrolyte potential, $u_{m,i}$ the ion mobility and u the velocity vector.

The three terms on the right-hand side represent the contributions of diffusion, migration and convection to the current density, respectively. For solutions containing an excess of supporting electrolyte, the ionic migration term can be neglected; if the electrolyte is well stirred and/or currents are kept so low that the electrode surface concentration do not differ appreciably from the bulk values, then ionic diffusion term can be neglected as well. Under these conditions,

the equation can be simplified, and becomes identical to Ohm's law.

The electrodes, usually metals, obey to the ohm's law and the current density vector can be defined thereafter, see equation 2.

At the interface, the electrode kinetics may have an impact on the overall potential and this is defined by the overpotential.

Thus we get these relations:

Electrode: $i_s = -\sigma_s \nabla \phi_s$, with conservation of current $\nabla . i_s = Q_s$ (2)

Electrolyte: $i_l = -\sigma_l \nabla \phi_l$, with conservation of current $\nabla . i_l = Q_l$ (3)

Electrode/Electrolyte interface:

$$\eta_m = \phi_s - \phi_l - E_{eq,m} \quad (4)$$

Where i_s stands for current density in the electrode, σ_s the conductivity of the electrode, ϕ_s the electric potential in the electrode, Q_s the general current source for the electrode, i_l stands for current density in the electrolyte, σ_l the conductivity of the electrolyte, ϕ_l the electric potential in the electrolyte, Q_s the general current source for the electrode, η_m the activation overpotential and $E_{eq,m}$ the equilibrium potential of a reaction.

The relation between current density and overpotential can be described by the Butler-Volmer or Tafel equations, and also by experimental data obtained from polarisation curves.

Aqueous based electroplating are usually governed by secondary current distribution. These implies that variation composition in the electrolyte are negligible and thus, that the electrolyte conductivity is uniform; also that the electrode kinetics, charge transfer, are taken into account.

For this specific application, these constraints are respected, as the electrolyte species concentrations are high, the electrolyte agitation is vigorous and the overpotential is small but not negligible.

3. Model creation

The description of the model follows the steps as defined in Comsol 4.4 [1].

The electrochemical cell design in Comsol starts by defining the model geometry. The three coupler components have a general 2 D axisymmetric geometry, but small although important features, make them fully 3D geometries.

In terms of physics, only electrochemical aspects were taken into account. As already justified in chapter 2, the chosen physics interface was Electrochemistry > Electrodeposition > Electrodeposition, Deformed Geometry > Electrodeposition, Secondary (edsec).

The chosen study was time dependent with initialisation.

3.1 Geometry

The geometry of each coupler subcomponent was processed individually and originated a dedicated Comsol study. This reflects also the reality for the copper plating as each component is also electroplated separately. The geometry was introduced into Comsol via STP file format (3D CAD) which wasn't originally simplified to be processed in Comsol. This implied a significant import post processing as can be seen in figure 1.

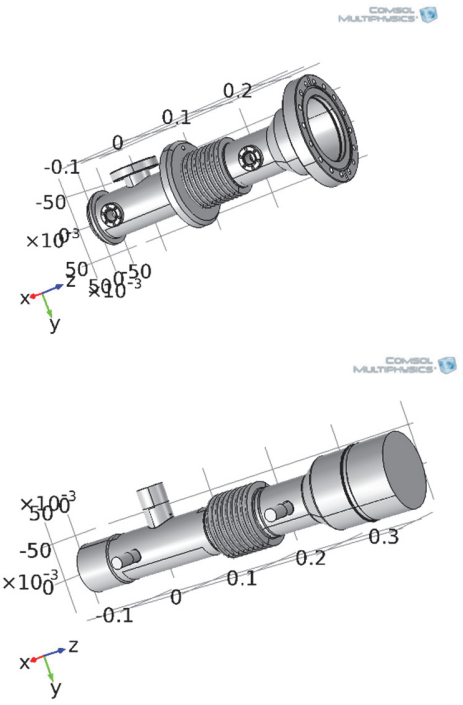

Figure 1: Coupler WEC subcomponent as imported (top) and post processing (bottom).

The following figure presents the two remaining coupler subcomponents geometries, already after the import post processing procedure. It concerns the CEC and the WIC subcomponents.

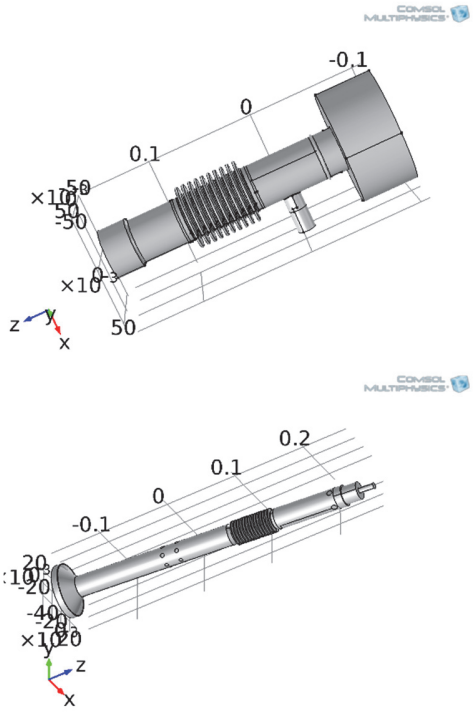

Figure 2: Coupler CEC (top) and WIC (bottom) subcomponents after import processing.

Coupler subcomponents define the cathode geometry, but still missing is the anode geometry. The main part of the simulation work performed with Comsol, was dedicated to the definition of the anode geometry capable of achieving the most even copper layer thickness for each different subcomponent; this will be described later on.

In terms of overall electrochemical cell geometry, there is a main difference between CEC, WEC and WIC; the plating surface of both CEC and WEC is the internal one and thus the electrochemical cell overall boundaries are defined by the subcomponent itself; however for WIC, where the plating surface is the external one, the overall boundaries were defined by the size of the existing electroplating tank.

3.2 Materials

All necessary information regarding materials specifications was directly integrated in the physics interface, namely the electrolyte conductivity.

3.3 Physics

Besides the default nodes of the electrodeposition secondary interface, two *External Depositing Electrode* nodes were added in order to set the boundary conditions for both the cathode and the anode. The main input value for the cathode was the boundary condition which was defined as the *Average Current Density*, also referred in this document as applied current density; this choice allows to see the working point on the cathodic polarisation curve (see figure 3) that was used to define the kinetics expression at the *Electrode Reaction* node (see equation 5). For the anode node, the inputs were given by one anodic polarisation curve and the boundary was set to *Electric Potential* and equal to zero.

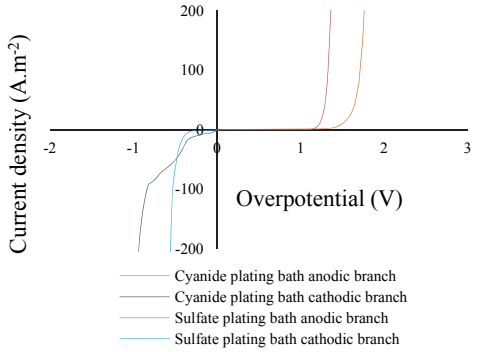

Figure 3: Polarisation curves from the two copper plating baths.

$$i_{loc} = int""(edsec.eta\_er1\left[\frac{1}{V}\right]) \qquad (5)$$

where: i_{loc} is the local current density; *int""* is the polarisation curve either for the cathode or the anode defined by an interpolation function of experimental data; *edsec.eta_er1* is the local overpotential as defined by Comsol.

The occurring chemical reactions are related to the two different copper plating baths. The first concerns a copper sulfate bath with the following composition:

$CuSO_4.5H_20$	75 g/l
H_2SO_4 (96%)	100 ml/l
Cl (NaCl)	0.075 g/l

This electrolyte has a conductivity of 22.6 $S.m^{-1}$, at room temperature. The cathodic reaction for this bath was considered to have a yield of 100% and can be described as:

$$Cu^{2+}_{(aq)} + 2e^- \rightarrow Cu_{(s)} \qquad (6)$$

Reduction of copper, with two electrons per copper ion. The anodic reaction concerns an

insoluble anode and thus the reaction can be described as:

$$2H_2O_{(l)} \rightarrow O_{2(g)} + 4H^+_{(aq)} + 4e^- \quad (7)$$

Oxidation of oxygen, with 4 electrons per oxygen molecule.

The second copper plating bath is a cyanide bath with the following composition:

CuCN	26 g/l
$NaKC_4H_4O_6$	60 g/l
Na_2CO_3	15 g/l
NaOH	12 g/l
NaCN	42 g/l

This electrolyte has a conductivity of 10.6 $S.m^{-1}$, at 45 °C. The cathodic reaction within the used current density was considered to have a yield of 100% and can be described as:

$$Cu^+_{(aq)} + e^- \rightarrow Cu_{(s)} \quad (8)$$

Reduction of copper, with one electron per copper ion. The anodic reaction is the same as the one for the copper sulfate bath.

3.4 Mesh

Depending on the geometry, the mesh settings went from Physics-controlled mesh with a normal to fine element size depending on certain fine features of the subcomponents geometry. Variations to finer mesh sizes had no relevant impact on the final results.

4. Results and discussion

The main objective of this simulation was to achieve a copper plated layer within the specified thickness tolerances for each of the three coupler components as defined hereafter:

Components	Minimum	Maximum
CEC	5 µm	15 µm
WEC	5 µm	15 µm
WIC	20 µm	40 µm

The two copper plating baths used in this work are the existing ones at CERN surface finishing workshop. The copper sulfate electrolyte has the advantage of being easy to operate, less toxic, with less drifts in terms of composition and working parameters, and also less prone to defects. Thus, the copper cyanide was introduced only when the copper sulfate failed to deliver complying results.

The copper cyanide electrolyte main advantage is its plating penetration, which is an advantage when working with complex geometries.

4.1 CEC anode geometry.

The starting anode geometry was a simple rod with an overall length of 194 mm (component length) and a diameter of 8 mm. The rod diameter starting value was defined by the available raw material.

Figure 4 presents the first results from simulation at different applied current densities for the copper sulfate plating bath. The figure presents two dotted horizontal lines which refer to the plated thickness tolerances; dark blue for the maximum thickness (15 µm) and light blue for the minimum thickness (5 µm). The orange line concerns the maximum copper layer thickness when the minimum thickness is achieved all-over the component surface; its value can be read on

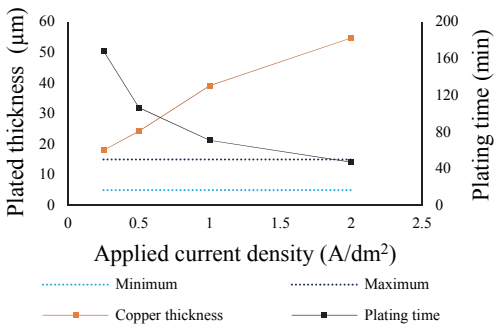

Figure 4: CEC plated thickness and plating time in function of the applied current density with the copper sulfate plating bath.

the left vertical axis. The black line shows the time taken to achieve the respective copper thickness; its value can be read on the right vertical axis. Time is an important parameter to take into account when transposed to production.

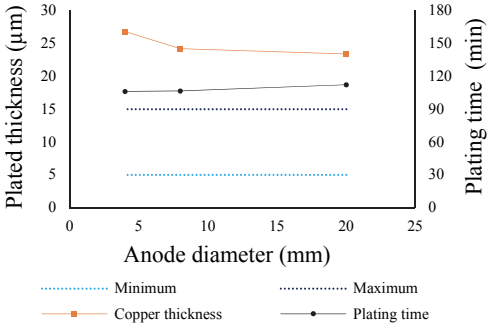

Figure 5: CEC plated thickness and plating time in function of the anode diameter at 0.5 A/dm^2.

This type of graphical representation is repeated several times in this document and its interpretation follows the same guidelines.

Figure 4 shows that a simple rod geometry wasn't able to respect the plated tolerances even at very low current densities; changing the rod diameter didn't make a big difference, see figure 5. No further effort was done concerning the rod diameter as it had also some practical implications regarding the supply of raw material.

The current density distribution graphic gave some tips on how to tackle the problem. Figure 6 shows a 3D representation of the current density distribution on the CEC component. Current density distribution is codified by a rainbow of colours going from dark blue (highest cathodic current densities) to dark red (lowest cathodic current densities). This graphic shows that for the simple rod anode, the current is mainly diverted to the straight parts of the component (blue surfaces). In order to better balance the current density distribution, the anode active surface close to these blue areas was reduced creating a higher resistance and thus, forcing the current to go elsewhere. Also, the anode length was increased to ease the flow of current towards the surface given by the big flange on the bottom.

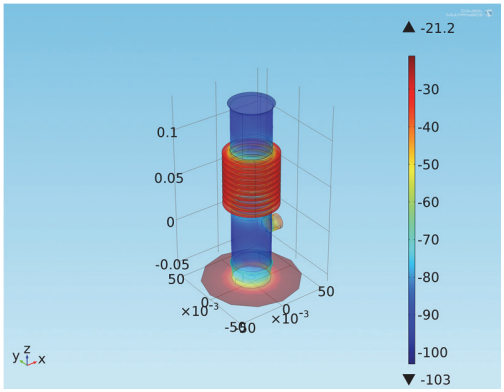

Figure 6: CEC current density distribution for an applied current density of 0.5 A/dm^2.

After some iterations to redefine the number and length of the different anode active areas, the achieved cathodic current distribution was improved significantly and the outcome is shown in figure 7. The range between the maximum and minimum current density values went from 81.8 to 40.6 A/dm^2; this gap reduction was mainly achieved on the higher current densities side.

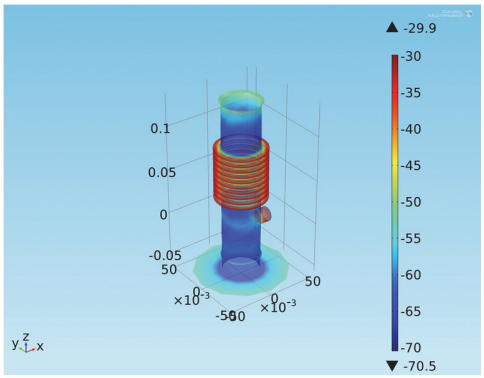

Figure 7: CEC current density distribution for an applied current density of 0.5 A/dm^2.

Figure 8 presents the simulation results obtained with the optimised anode geometry, with the plated thickness and time at different current densities. Comparing with the data acquired using a simple rod anode (see fig. 4), the improvement is clear.

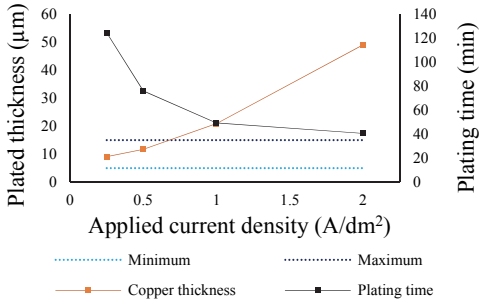

Figure 8: CEC plated thickness and plating time in function of the applied current density for the optimised anode geometry.

The new anode shape allows not only to get within the specified plated thickness, but also to reduce the time needed to achieve it. From figure 8, it's possible to get the best applied current density and that would roughly be slightly below 0.7 A/dm^2 with a plating time slightly above 60 minutes. This optimum value is defined through the intersection of the line defined by the extrapolation of the copper plated thickness values with the maximum copper thickness tolerance value.

4.2 WEC anode geometry.

The approach for the WEC component was quite similar to the CEC and thus, only the final results are presented hereafter. In figure 9 is

possible to see the corresponding current density distribution for the optimised anode geometry.

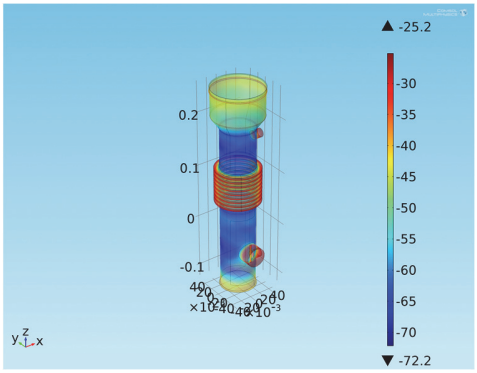

Figure 9: WEC current density distribution for an applied current density of 0.5 A/dm^2.

In figure 10 is represented the plating thickness and time for the optimised anode at different applied current densities. For the WEC component the optimum working current density lies slightly below 0.5 A/dm^2 with a plating time of 90 minutes.

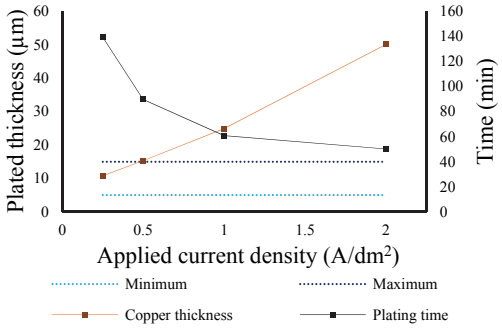

Figure 10: WEC plated thickness and time in function of the applied current density for the optimised anode geometry.

4.3 WIC anode geometry.

As already mentioned for the WIC component, a different approach was adopted due to the fact that the surface to be plated is the external one. This made possible the exploitation of the existing plating tank without a need to define an auxiliary anode, as it was the case for the CEC and WEC components.

The simulation was done by modelling the existing plating tank and anodes geometry. The first observation from simulations was that the relative position of the component towards the anodes as well as the number of anodes had little or no impact in the current density distribution. The second evidence from simulations was that the copper sulfate bath wasn't able to get the copper layer thickness within specifications without going to very low current densities and thus, very long plating times; an auxiliary anode would certainly improve results but at the expense of a more complex setup. This solution path wasn't explored since a cyanide copper bath was also available in the workshop and that would in principle be in situation to improve the result achieved with the copper sulfate bath.

Although harder to operate, the copper cyanide bath is known for its ability in achieving more uniform plated layers, at least if compared with the copper sulfate without additives. Thus, the copper cyanide bath was taken into account and simulation data gave indeed much better results towards the specified tolerances. In figure 11, it's possible to see the results obtained with the two plating baths for different current densities. The copper cyanide bath has an optimum slightly above 0.5 A/dm^2 with a plating time around 120 minutes; in contrast to the copper sulfate bath, that has an optimum slightly above 0.25 A/dm^2 for a plating time of 500 minutes. The improvement in the plating time is justified by the higher current density and by the fact that the cyanide bath has the double plating speed for the same current density as it only requires one electron to reduce a copper ion, instead of two as in the case of the copper sulfate bath; also assuming that both reactions have a 100% yield.

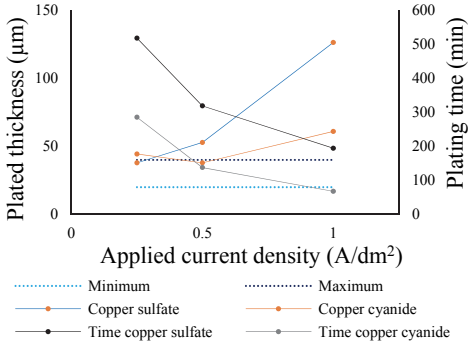

Figure 11: Plated thickness and time in function of the applied current density for the copper sulfate and copper cyanide baths.

5. Conclusions

The work developed with Comsol allowed to evaluate the feasibility of plating complex geometries such as the ones of the couplers subcomponents. The data acquired from the

different simulations allowed to: chose the most interesting operating bath; define, within a few iterations, an optimum working geometry for the CEC and WEC anode; define, the optimum working parameters, current density and plating time. It allowed, altogether, to achieve the specified copper layer thickness within tolerances.

Concerning the WIC geometry, simulation data showed that the copper sulfate plating bath wasn't able to respect the specified copper layer thickness specifications without long plating times; on the other hand, the copper cyanide bath, was capable of doing it within the existing bath and anodes setup.

6. References

1. http://www.comsol.com/electrodeposition-module